# EFFECT OF DYNAMIC LOADING ON COMPRESSIONAL BEHAVIOR OF DAMPING CONCRETE

**E. Kasparek** **R. Scheidemann**

**U. Zencker** **D. Wolff** **H. Völzke**

BAM Federal Institute for Materials Research and Testing
Berlin, Germany

## ABSTRACT

In drop test scenarios related to assessing and licensing the storage procedure of spent fuel and high active waste, the casks under examination are generally not equipped with impact limiters. Hence, the extent of mechanical stresses in case of an assumed handling accident is largely affected by the ground properties of the reception hall floor in the specific storage facility.

Unlike conventional brittle foundation materials, damping concrete performs quite well in such applications as it features high stiffness as well as high energy absorption due to the filler pore volume. However, its damping ability is not sufficiently exploited in current finite element (FE) calculations due to a lack of advanced material models for simulating its impact response. An implementation of qualified concepts that account for plastic, strain rate dependent behavior requires additional information that has to be provided by systematic test series.

BAM recently started a research project to generate such data, subsequently to develop and to improve numerical methods for the analysis of impact limiters and damping foundation material and thus to optimize safety assessment tools for the design of transport and storage casks. A major part of this research concerns dynamic compression tests of variably shaped specimens conducted at a servo hydraulic 1MN impact testing machine as well as at a BAM facility for guided drop tests. This presentation focuses 100mm damping concrete cubes deformed vertically at constant rates under different constraint conditions. For example, a special fitting jig was constructed to subject the specimens to multi-axial loading. Thereby a deformation of 60% could be applied.

Simulation was conducted by FE code ABAQUS™ based on material models “Concrete damaged plasticity” and “Crushable foam” which both allow defining rate sensitive nonlinear stress-strain relations in compression beyond the classic metal plasticity approach.

## INTRODUCTION

Casks for high active waste and spent fuel are usually equipped with impact limiters at bottom and lid end during transport, whereas these structures are removed after unloading of the transport vehicle in the reception hall of storage facilities. Thus, appropriate foundation materials are needed that feature both high stiffness and considerable energy absorption capacity to limit possible cask loads in case of an assumed handling accident. As conventional concrete inherently has only poor damping abilities, the German company HOCHTIEF®, which is an international provider of construction-related services, developed a new mixture by adding polystyrene balls as filler.. For application as material for ground floors in German interim storage facilities, test results are

available from the manufacturer. An extension of the pool of experimental data to even higher strain rates is desirable to fully take advantage of expected further damping capabilities. With regard to inevitable simplifications when simulating such impact scenarios and to the consequently conservative design, BAM incorporated systematic investigations of damping concrete as part of research project “Development of numerical methods for analyzing impact limiters subjected to impact or drop scenarios (ENREA)”. Latter is aimed to develop and to improve numerical methods for simulating impact limiting components based on an extensive experimental program that involves nearly 1000 specimens made of wood, foam and concrete. This paper focuses on displacement-driven compression tests at variable loading speeds, temperatures and boundary conditions which were carried out on damping concrete cubes. The sections below address the relevant experimental set up, the test output and results of respective numerical simulations. The current work shall firstly clarify the question whether concrete material models provided by FE code ABAQUS™ are suitable to reproduce all relevant properties to be observed in laboratory.

## TEST PROGRAM

The experimental program of the past project phase comprises five different test series at ambient temperatures with and without constraints to lateral expansion. Each test series consists of a preliminary test and five regular tests and is denoted by a two-part identifier indicating the boundary conditions and the stamp speed (Table 1). The loading rate, ranging from 0.02mm/s to 3000mm/s, is constantly applied until the machine reaches its maximum load or until complete failure. While latter condition is limited to uniaxial experiments, all other specimens were subjected to an average of 55mm displacement yielding a true deformation of 125% with regard to the initial height of 100mm.

**Table 1. Classification of test series**

| | loading rate | | |
|---|---|---|---|
| | D1=0.02mm/s | D2=200mm/s | D3=3000mm/s |
| unconstrained | U_D1 | -- | U_D3 |
| constrained | R_D1 | R_D2 | R_D3 |

The tests are realized by means of a servo-hydraulic 1MN impact machine. The axial load can be measured at top and bottom of the specimen by a load cell and a strain gauge instrumented pressure stamp . In order to reduce friction, Teflon spray was employed at the specimen-platen interface. It was likewise applied to the inner side walls of the jig holding the sample when performing experiments imposing zero in-plane strain. This device, which is shown in Figure 1, allows easy replacement of specimens and adoptions to their geometrical tolerances due to its movable parts. Two of the perpendicular bolts pressing the side walls against the specimen are provided with a central bore for receiving a cylindrical strain gauge which records forces in lateral x- and y-directions (Fig. 2). A laser-displacement-sensor based on a triangulation principle and thus determine straightforward the distance between the stamp and the specimen support discarding the flexibility of the overall equipment. In principle, the whole measuring system operates at adaptable sampling rates which account for the broad variation in duration of the loading procedure.

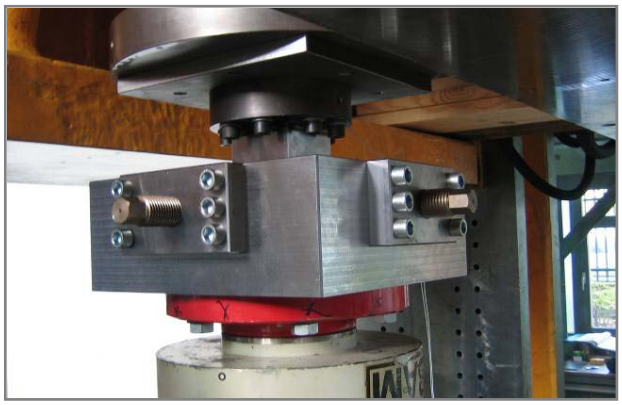

**Figure 1. Holding jig for laterally constrained specimens**

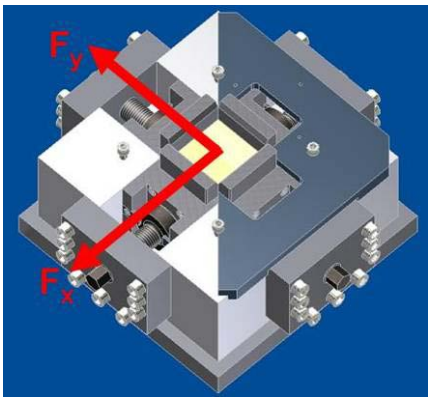


**Figure 2. Lateral force measurement**

## TEST RESULTS

Tests with lateral constraints

The output of every single experiment encompasses time series of the relative stamp displacement, of axial forces as well as of lateral forces in x- and y- directions. The corresponding stress-strain-relations are generated by referring these data to the particular dimensions of the loaded specimen. In Figure 3 the resulting axial stress-axial strain functions are given for tests under quasi-static loading (test series R_D1), while Figure 5 depicts these relationships for highly dynamically loaded specimens (test series R_D3). All curves exhibit a similar behavior characterized by a short elastic range and an extensive compaction zone with low strain-hardening followed by densification that arises at a strain level of approximately 75% to 100%. A more detailed look at the low strain region reveals an additional zone: just after the elastic peak stress, strength abruptly reduces by half. However, the related steep softening can only be identified for quasi-static loading (Fig. 4), while this effect vanishes for increasing loading speed (Fig. 6).

In order to quantify the dynamic hardening of damping concrete, the mean stress-strain curves for different loading rates are compiled in Figure 11. Both the increase of loading speed from 0.02mm/s to 200mm/s and from 200mm/s to 3000mm/s result in a significant increase of strength. With respect to the quasi-static stress curve, the values are scaled up by approximately 20% (R_D2) and 40% (R_D3). As the distances between these three curves do not correspond to the distribution of the corresponding mean strain rates on a logarithmic scale (Fig. 7), rate sensitivity can not be captured by a standard approach.

If such an evaluation is rather drawn on integral values, the findings are only slightly different. Table 2 presents the area under the mean stress-strain curves for all three test series. In addition a statistical t-test is performed to investigate the separation of these values, i.e. to describe the probability (p-value) that a curve belonging to a specific test series can be related to the mean stress curve of test series with a higher loading rate. This test incorporates the standard deviations of the integral values, which vary between 5.1% and 6.7% and do not show any systematic rate sensitivity. The p-values evaluated for test series R_D1 versus R_D2 and R_D2 versus R_D3 are very low, thus ascertaining the dynamic hardening of damping concrete, but they differ by one order of magnitude. Consequently, the speed increase from 0.02mm/s to 200mm/s is regarded to cause a considerably larger effect compared to a further increase up to 3000mm/s.

Due to the fact that lateral stress curves of the same test series show similar deviations as axial stress curves, just averaged values are going to be presented here. Furthermore, the arithmetic mean

is formed by adding data from x- and y- direction thanks to their effectual consistency. The resulting figures are related to the respective axial stresses (Fig. 8). It is to summarize, that relevant lateral stresses develop in the plastic zone, reach one third of the axial stresses at a strain level of 50% and continue asymptotically in the densification regime. Although at first sight these relationships appears to be strain rate sensitive, the data collected so far is not sufficient to set up a qualified formulation. In fact, experiments with additional strain rates are needed to ascertain this assumption.

**Table 2. Statistical quantities for comparing σ-ε-integral between different test series**

| | R_D1 | R_D2 | R_D3 |
|---|---|---|---|
| Integral σ-ε (mean) | 26.26 MPa | 33.05 MPa | 38.22 MPa |
| Standard variation | 5.1% | 6.7% | 6.6% |
| | D1▶D2 | D2▶D3 | |
| Increase of integral | 25.8 % | 15.6 % | |
| p-value | 0.02 % | 0.37 % | |

Uniaxial tests

Unlike in the previous chapter, the stress values presented for uniaxial experiments are not related to the actual cross-section of the specimen due to its unrecorded deformation in the plane. Hence, the function of nominal axial stress versus logarithmic axial strain is given exemplary for test series U_D1 (0.02mm/s) in Figure 9. An elastic peak occurs at approximately 1% strain, followed by strain-softening and a minor stress increase prior to complete failure. Data beyond 2% strain rather describe the response of the machine to the specimen collapse. Considering the fast failure, deviations from true stresses can be neglected, which allows to compare stress curves for different boundary conditions focusing the low strain zone (Fig. 10). It turns out that the elastic range of unconstrained specimens is larger, leading to a higher elastic peak stress due to similar elastic modulus. This observation holds especially for dynamically loaded bodies.

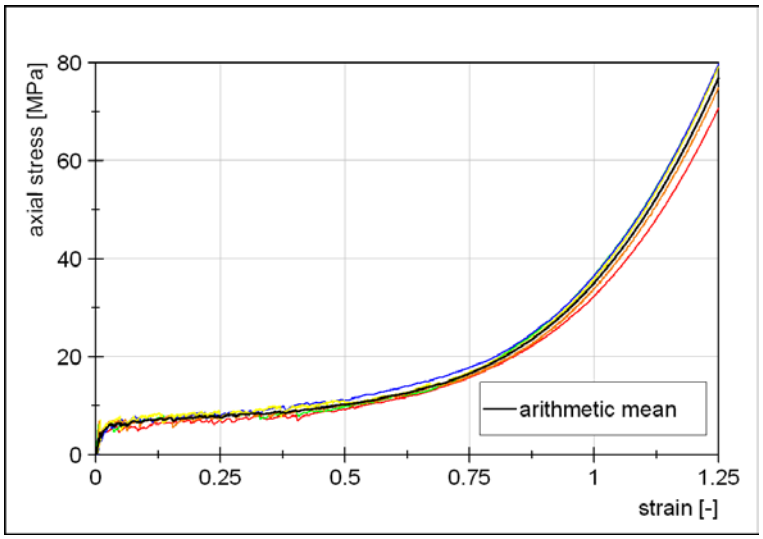


**Figure 3. Stress-strain relations for test series R_D1 (speed = 0.02mm/s)**

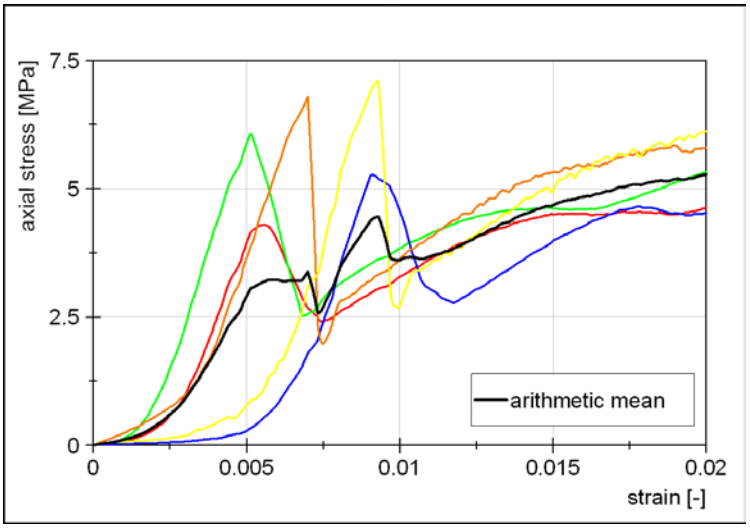


**Figure 4. Excerpt of stress-strain relations for test series R_D1 (speed = 0.02mm/s)**

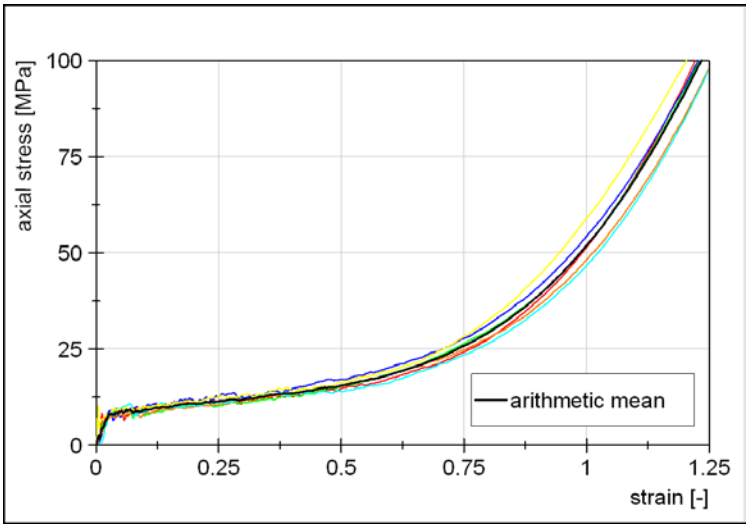


**Figure 5. Stress-strain relations for test series R_D3 (speed = 3000mm/s)**

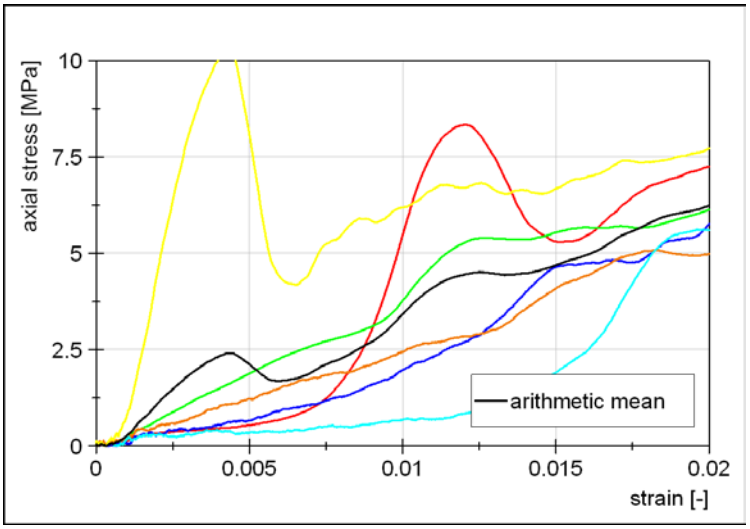


**Figure 6. Excerpt of stress-strain relations for test series R_D3 (speed = 3000mm/s)**

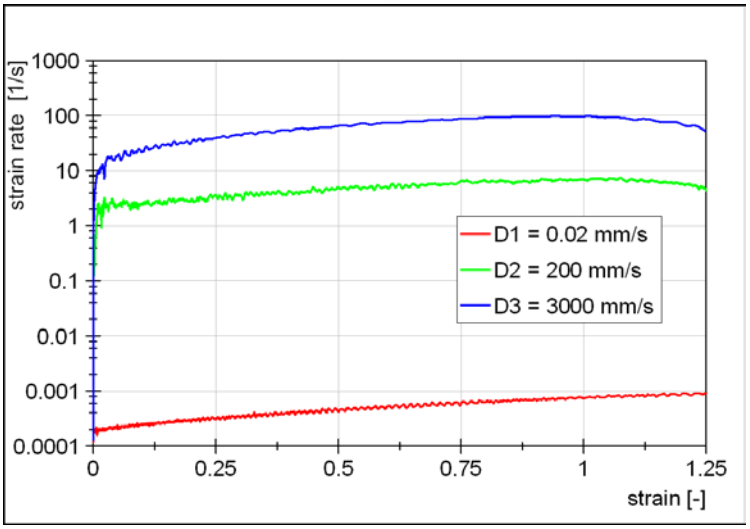


**Figure 7. Mean strain rates for test series R_D1, R_D2 and R_D3**

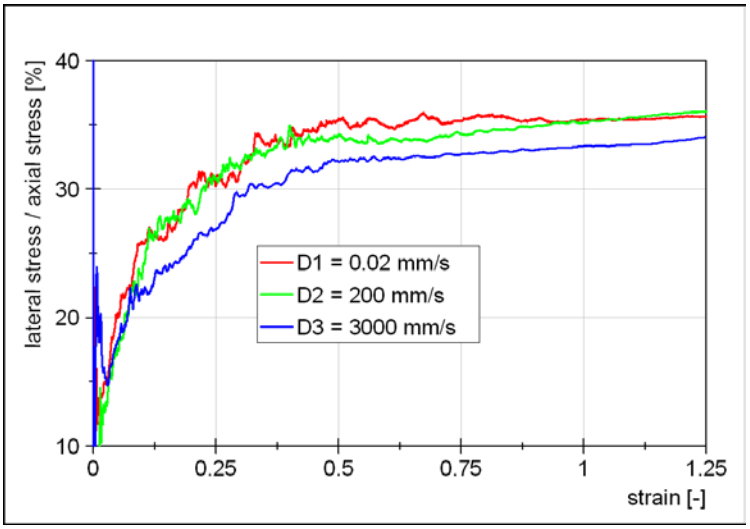


**Figure 8. Mean fractions of lateral versus axial stresses for test series R_D1, R_D2 and R_D3**

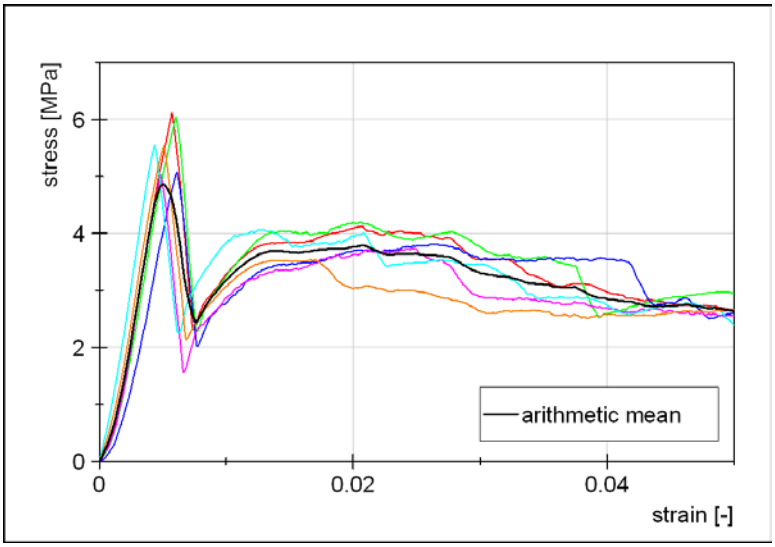


**Figure 9. Stress-strain relations for test series U_D1 (speed = 0.02mm/s)**

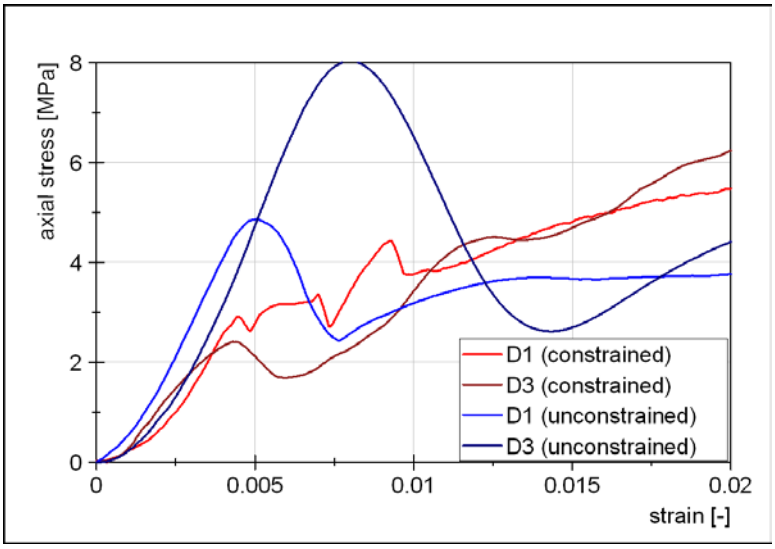


**Figure 10. Mean stress-strain relations for test series R_D1, R_D3, U_D1 and U_D3**

## NUMERICAL ANALYSIS

The following numerical investigations are aimed to evaluate whether conventional material models provided by ABAQUS library can reproduce the behavior of constrained specimens at varying loading rates. A rather simplified finite element representation of the testing facility proved to be advantageous since it facilitates to systematically and efficiently trace the impact of individual material parameter on the response. Hence, just one eight of the specimen was modeled assuming symmetry amongst others between specimen top and bottom, while jig and stamp were considered to be rigid. Additional experiments on well-known reference materials were performed to provide benchmark data for validating major model input such as friction coefficients and mesh size.

Eventually, simulations based on the material model “Crushable foam” for aluminum alloys developed by Deshpande and Fleck [1] were performed. Apart from softening in the low-strain zone, which can’t be reproduced by this approach, a good agreement with experimental results were achieved (Fig. 11). Dynamic hardening was covered by scaling the applied quasi-static yield curve, which is likewise given in Fig. 11, with factor 1.2 for strain rate 3/s and 1.4 for strain rate 50/s. Anyhow, a successful application to realistic impact scenarios is subject to the dominance of multiaxial compression. If such conditions are met even in the transition area of the strike is going to be studied in upcoming drop tests. A more powerful concept dedicated to concrete under tensile and compression was described by Lubliner [2] and implemented in the material model “Concrete damaged plasticity”. Hereby development of plastic deformation is predominantly controlled by strain dependent damage variables, which allow simulating likewise strain-softening and strain-hardening. However, the cohesion-oriented model does not appropriately account for triaxial compression states as this is the only stress configuration without an eventual complete loss of strength. Consequently the calculations failed in simulating the whole densification zone whereas good results are delivered for the low strain region even for different strain rates. These results indicate a need to extend the model from Lubliner which can be done by modifying the yield criterion.

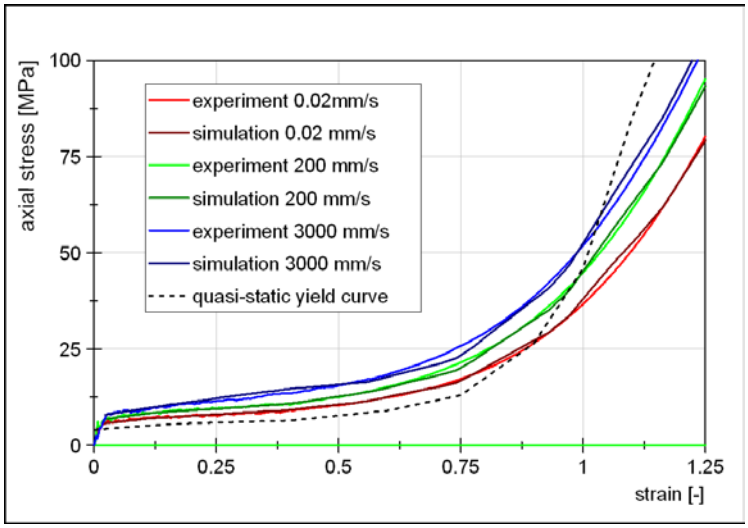


**Figure 11. Mean experimental stress-strain curves and numerical results for test series R_D1, R_D2 and R_D3**

## CONCLUSIONS

The experimental results of compression tests on damping concrete cubes identified a significant strain rate dependency for constrained and unconstrained conditions. In case of multiaxial compression states the stress-strain relations yield an extensive compaction zone with low-strain hardening followed by densification at a strain level of approximately 75%. Due to the high agreement with the behavior of cellular materials, material models dedicated to foam can be applied in numerical simulations. However, they can not reproduce strain-softening which is considered to have an important influence on the response in realistic impact scenarios which will be studied in further test series. As the concrete model from Lubliner featuring damage variables that are required to incorporate the loss of strength, failed in simulating the densification zone, an extension of the yield criterion and implementation of this modification is the next challenge to be met.

## ACKNOWLEDGMENTS

The research project ENREA (Development of numerical methods for analyzing impact limiters subjected to impact or drop scenarios) is sponsored by the German Federal Ministry of Education and Research under contract no. 02S8588.

## REFERENCES

[1] V.S. Deshpande, N.A. Fleck, Isotropic constitutive models for metallic foams, J. Mech. Phys. Solids vol. 48 (2000), no. 7, 1253-1283.

[2] J. Lubliner et al., A plastic-damage model for concrete, Int. J. Solids Structures vol. 25 (1989), no. 3, 299-325.